Low Temperature Physics/Fizika Nizkikh Temperatur, 2021, vol. 47, No. 12, pp. 1090–1095

Probing long-range current-carrying edge modes by two quantum point contacts

M. Belogolovskii and E. Zhitlukhina

Donetsk Institute for Physics and Engineering named after O. O. Galkin of NAS of Ukraine, Kyiv 03028, Ukraine
E-mail: belogolovskii@ukr.net

P. Seidel

Institut für Festkörperphysik, Friedrich-Schiller-Universität Jena, Jena 07743, Germany

Received July 8, 2021, published online October 25, 2021

The origin of anomalous current-carrying edge states in quasi-two-dimensional quantum samples with an insulating interior is currently mysterious. We propose to address this issue using a hybrid setup, an interferometric phase-sensitive configuration of two independent scanning probe tips, normal and superconducting, able to realize the quantum interference effect of quasiparticle currents moving in different directions along the metallic-like one-dimensional near-boundary channels. To simulate the dissipationless edge currents, we consider a quantum material with a simple Corbino disk geometry and analyze how the differential conductance spectrum depends on the distance between the two tips, the applied voltage bias, and the presence of a magnetic field. An essential difference between classical and quantum expectations should clarify the enigmatic origin of the long-range conducting modes observed in different materials at low temperatures. Strong dependence on the applied magnetic field can be useful for practical implementation of the quantum effects associated with the phase difference of electron wave functions in the ring geometry.

Keywords: helical edge currents, Corbino disk, two-probe contact setup, differential conductance spectrum.

1. Introduction

Electron correlations and topology are well known as physical phenomena leading to surprising and potentially functional properties. The integer quantum Hall phenomenon, a quantized version of the classical Hall effect discovered in 1980 and observed in two-dimensional electronic systems subjected to strong magnetic fields and ultra-low temperatures, was the first condensed matter phenomenon exhibiting topological features [1]. In the conventional quantitative interpretation, bulk electrons, under the influence of the magnetic field, are confined to small circular orbits while those, whose wave functions are squeezed toward the system's boundaries, are moving along them. The number of such modes known as "edge states" is determined by the Chern number. Subsequent search for other topological electronic phenomena discovered them in seemingly ordinary bulk materials under non-extreme conditions, which led to a real revolution in understanding the ubiquitous topological structure of quantum matter [2]. It was found that topological materials with strong correlations usually exhibit orbital and/or spin ordering with intrinsic magnetic, orbital, or electronic anisotropy. In particular, a remarkable class of novel materials known as topological insulators display unique symmetry-protected helically propagating edge modes with an insulating interior. Depending on the material symmetry and its dimension, such exotic states may be either spinless or spinful, thus contributing to the emergence of gapless edge/surface charge or spin currents.

Following theoretical progress in this field and prediction of various topological insulators in two and three dimensions, the realization of topological states experimentally and probing of the edge currents have been intensively developed [3]. There was quite a lot of evidence that at very low temperatures, non-dissipative currents arise at the interface between two topologically distinct phases explained as topologically protected edge currents. Nevertheless, there are more and more indications that such conducting channels may also have a non-topological nature. Such trivial (from the topology viewpoint) edge states should arise in the situation when the chemical potential resides within the band gap in the material bulk, but is pinned in the conduction band on the surface. For example, such scenario was realized in InAs Josephson junctions, see the paper [4] and references therein to some related works dealing mainly with doped semiconductors.

Recently, the presence of unexpected non-topological currents was revealed in other materials, where their origin is, most probably, different. For example, by investigating proximity-induced superconductivity and comparing normal-state measurements in the Hall bar and Corbino geometries, the authors [5] proved the presence of metallic-like edge conductance in gapped graphene and attributed it to a non-trivial topology of the gapped Dirac spectra. However, according to the recent paper [6] dealing with a charge-neutral graphene, the observed one-dimensional transport has no topological origin, but rather is related to commonly occurring charge accumulation at graphene edges. Moreover, it was found that the edge conductance has little effect on the current flow at zero magnetic field but leads to field-induced decoupling between edge and bulk transport at moderate fields [6]. Quite surprising results [7] were recently obtained for the Kondo insulator SmB_6, namely, unexpected quantum oscillations in the insulating state, immune from the disorder bulk, and correlation-driven non-dissipative helical modes, which are expected to be topologically protected by time reversal symmetry physics. At the same time, the authors [7] found conducting one-dimensional channels perpendicular to the surface, which are unusually resistant to scattering and end at the edges of the surface steps. But most exciting was their presence even at room temperature, indicating unconventional physics in the SmB_6 compound [7].

The last two examples [6, 7] demonstrate the need for a detailed study of intrinsic edge currents in various exotic materials using well-developed experimental techniques as it was done in the paper [6] by applying the SQUID-on-tip approach or in the work [7] by using the scanning microwave impedance microscopy. What we propose for probing long-range conducting edge modes is an interferometric phase-sensitive setup consisting of two independent tips, normal and *s*-wave superconducting, a simpler but efficient methodology (Fig. 1). We show that such device is able to realize quantum interference effect of quasiparticle excitations moving in opposite directions along metallic-like one-dimensional edge channels and therefore, it can be useful for revealing the origin of anomalous conducting edge states in quantum materials. Next, we discuss the fundamental ideas and measurable implications of the proposed approach.

2. Theoretical model

Following Laughlin's heuristic reasoning that he put forward shortly after experimental discovery of the integer quantum Hall effect, we limit ourselves by a two-dimensional Corbino disk with a uniform density of mobile carriers in the quantum Hall effect plateau (Fig. 1). To calculate the current vs voltage curves for such setup, we use our general scattering-like approach to transport characteristics of a superconductor-based device coupled to two electron reservoirs characterized by their chemical potentials μ_L and μ_R [8] and that developed for an electron current through a nanoscale phase-coherent quantum ring [9]. In this work, we combine the two approaches into a single methodology.

Let us imagine a two-terminal one-dimensional structure formed by three main elements, a normal tip N with incoming electrons, complex normal-state device O, and an *s*-wave superconducting tip S with an isotropic energy gap Δ. We introduce an additional infinitesimal normal section n between the ring and the S electrode. Then the device O that is assumed to be quantum-coherent and bounded by points 1 and 2 is composed of two Y-shaped splitters with their own scattering matrices shown separately on both sides of Fig. 1 and the one-dimensional quantum ring itself.

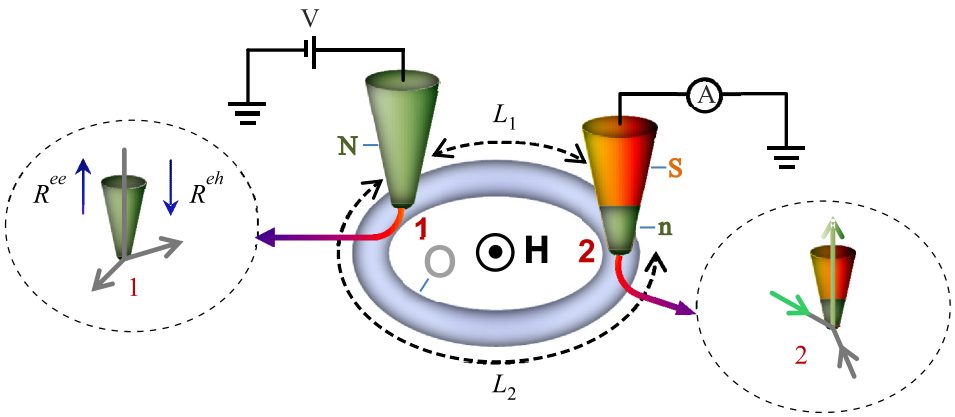

Fig. 1. (Color online) Illustration of the experimental setup with two tips, normal (N) and superconducting (S), for probing long-range edge currents in a Corbino disk. Two highlighted areas exhibit the presence of two splitters. The character of the charge transmissions across the nanoscale ring can be studied by changing their mutual arrangement and scanning over the voltage V from zero to $2\Delta/e$, Δ is the superconductor energy gap. Other details are explained in the text.

The current I across the heterostructure is the same in all series-connected parts of the setup, hence, we may calculate it in a wire connecting the left reservoir with the tip N. For an electron entering the system from the left reservoir there are two possibilities, to be scattered back as an electron with the probability amplitude $R^{ee}(\varepsilon)$ or as a hole with the probability amplitude $R^{eh}(\varepsilon)$. Then the conductance spectra $G(V) = dI(V)/dV$ of the entire structure read as [10]:

$$G(V) = \text{const}\left[1 - R^{ee}(\varepsilon = eV) + R^{eh}(\varepsilon = eV)\right], \quad (1)$$

where $\varepsilon = E - E_F$, E is the electron energy, E_F is the Fermi energy, $V = (\mu_L - \mu_R)/e$ is the voltage bias. The constant factor in Eq. (1) can be eliminated by multiplying $G(V)$ with resistance R_N of the whole setup transferred into a normal state.

Following the work [8], we interpret the charge transmission across the N-O-n/S setup as a sequence of an infinite number of interface scattering events including Andreev electron-hole and vice versa transformations at N/S boundaries:

$$R^{eh} = t_O^e r^{eh} t_O^h \left(1 + r_O^{h\leftarrow} r^{he} r_O^{e\leftarrow} r^{eh} + \ldots\right)$$

$$= t_O^e r^{eh} t_O^h / \left(1 - r_O^{h\leftarrow} r^{he} r_O^{e\leftarrow} r^{eh}\right);$$

$$R^{ee} = r_O^{e\rightarrow} + t_O^e r^{eh} r_O^{h\leftarrow} r^{he} t_O^e \left(1 + r_O^{h\leftarrow} r^{he} r_O^{e\leftarrow} r^{eh} + \ldots\right)$$

$$= r_O^{e\rightarrow} + t_O^e r^{eh} r_O^{h\leftarrow} r^{he} t_O^e / \left(1 - r_O^{h\leftarrow} r^{he} r_O^{e\leftarrow} r^{eh}\right). \quad (2)$$

Here $t_O^{e(h)}$ are probability amplitudes for an electron e or a hole h transmitted across the normal-state O device, $r_O^{e(h)\rightarrow}$ and $r_O^{e(h)\leftarrow}$ are probability amplitudes for quasiparticles arriving from the tip N ($\rightarrow$) and the tip S ($\leftarrow$) and scattered back from the O region. The amplitudes r^{eh} and r^{he} describe Andreev-retroreflection processes when an electron (hole) incident on the n/S interface from the O side is scattered back into a hole (electron) state, respectively. The latter events by which normal current is transferred to a supercurrent are characterized by amplitudes $h(\varepsilon) = \text{sgn}(\varepsilon)\sqrt{\varepsilon^2 - \Delta^2}$ for $|\varepsilon| > \Delta$ and $h(\varepsilon) = i\sqrt{\Delta^2 - \varepsilon^2}$ for $|\varepsilon| < \Delta$, see the overview [10].

In each splitter, we introduce coordinates x_n (n = 1, 2, 3) increasing from the nodes where they become zero. At these points, incoming quasiparticle wave functions, which are carrying unit flux $\psi_n^{(\text{in})}(x_n) = \left(m/\hbar\sqrt{k_n}\right)\exp(-ik_n x_n)$ with a quasielectron mass m, are entangled and together with outgoing waves form the wave functions $\psi_n(x_n)$ in each branch. The difference between holes and electrons in the amplitudes $t_O^{e(h)}$, $r_O^{e(h)\rightarrow}$, and $r_O^{e(h)\leftarrow}$ originates from the distinction between their wave numbers that grows as the quasiparticle energy ε increases above the energy gap Δ. $k^{e(h)}(\varepsilon) = k_F \pm \varepsilon/\left(\hbar v_F\right)$, k_F and v_F are Fermi wave number and velocity, respectively. The complex-valued phase shift acquired during an electron (hole) path between the points 1 and 2 controls the shape of the $G(V)$ curve. An impact of the inequality $k^e(\varepsilon) \neq k^h(\varepsilon)$ depends on the value of the dimensionless parameter $\eta = L\Delta/\left(\hbar v_F\right)$. It is extremely small when $\eta \ll 1$ and starts to play an important role when $\eta \leq 1$, see below.

Scattering parameters t_O^e, $r_O^{e\rightarrow}$, and $r_O^{e\leftarrow}$ for electrons were found in the work [9] using modified Griffith boundary conditions at the junction nodes. Their generalization to the case of holes is trivial. In the external magnetic field, electrons and holes propagating along a loop from the left to the right node pick up an additional phase $\pm 2\pi\Phi L_{1,2}/(\Phi_0 L)$ depending on the carrier charge and a clockwise or anticlockwise motion in the two segments of the loop with lengths L_1 and L_2, see Fig. 1. The sum $L = L_1 + L_2$ is the loop circumference, $\Phi_0 = h/e$ being the elementary flux quantum. If the device is perfectly quantum-coherent, there is an infinite number of internal reflections and transmissions inside the loop. They can be summarized using the conventional matching procedure, see the details in the paper [9]. In the next section, we present our numerical results emphasizing the difference between quantum (ballistic) and classical (dissipativen) regimes of the charge flow through the two-dimensional Corbino disk.

3. Numerical results

The voltage V applied to the setup generates the charge flow across it. The presence of an S tip strongly enhances sensitivity of the conductance spectra $G(V)$ to the charge transmission regime across the O region. As is well known for N–barrier–S trilayers [10], with increasing the barrier transmission probability, the shape of the differential conductance $G(V)$ changes from two prominent peaks at $|V| = \Delta/e$ (the tunneling regime) to a flat section increased up to two times conductance at $|V| < \Delta/e$ (the point-contact regime). As is explained below, a similar transformation is expected for our setup when conditions for an almost ideal transmission $t_O^{e(h)} \leq 1$ through the structure are violated. This is possible if the parameter η cannot be neglected or when an external magnetic field **H** is switched on, see below.

Let us start with the calculations for very small parameters η and missing magnetic fields. The first condition means that we may ignore the difference between momenta of electrons and holes with the same energy and take into account only the difference in their charges. This corresponds to ultra-small rings made of conventional metals with a relatively high Fermi velocity v_F. Our calculations show that in this case, the conductance spectrum does not depend on the position of the S tip, and its shape is very similar to that for a point contact formed by a normal tip with a superconductor. This result is strange from the viewpoint of the classical theory of electrical circuits. Indeed, if two arms of a classical loop have different resistances, the total resistance is a function of their ratio and the current

across a voltage-driven ring should depend on the position of a moveable tip. In quantum devices, the currents are determined by boundary conditions, hence, must match. If the transport conditions in the two arms differ (for example, their lengths are unequal), then (even in the absence of a magnetic field) persistent currents I_0 are circulating along the quantum ring. In this case, the total flow of incident carriers I splits into two different components in the arms $I_1 = I/2 + I_0$ and $I_2 = I/2 - I_0$, see [11] and references therein. The inset in Fig. 2 shows how their difference $\delta I_0 = (I_1 - I_2)/2(I_1 + I_2)$ is modifying with a change in the ratio between the two lengths $\delta L = (L_1 - L_2)/(L_1 + L_2)$. The presence of a persistent current provides independence of the final characteristic $G(V)$, measured outside the ring, on the superconducting tip position. Its shape can be seen in Fig. 2(a).

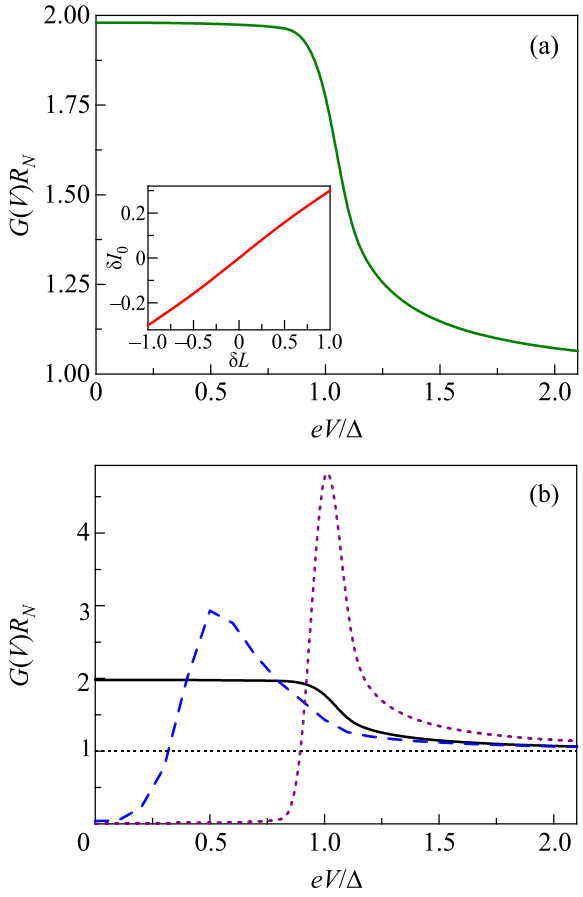

Fig. 2. (Color online) Conductance spectra $G(V)$ of a quantum loop shown in Fig. 1 without (a) and in the presence (b) of an external magnetic field **H**, the Fermi momenta for electrons and holes are assumed to coincide ($\eta \ll 1$). At $H = 0$, the $G(V)$ curve does not depend on the S tip position. At $H \neq 0$, the magnetic flux Φ through the ring equals to 0, $0.01(h/2e)$, and $0.1(h/2e)$ (solid, dashed, and dotted lines, respectively), R_N is the resistance of the same setup in the normal state, Δ is the energy gap of an *s*-wave superconducting tip, $L_1 = L_2$. Fermi wave numbers for the metallic loop are twice those for the tips. The inset demonstrates δI_0 vs δL dependence.

The magnetic flux Φ threading the ring breaks time-reversal symmetry, realizing a preferable direction for the charge flow. In this way, it destroys a compensating character of the persistent currents and, as a result, a part of the electron flux entering the N tip from the left reservoir is reflected back. Such retroreflection is similar to the barrier effect and, as a result, $G(V)$ curves for nonzero magnetic fields shown in Fig. 2(b) resemble conventional characteristics of superconductor-based trilayers with a tunnel barrier [10].

Let us transfer to the case when the difference in the Fermi momenta for electrons and holes is important, for example, in doped semiconductors with relatively small Fermi velocity. Figure 3(a) exhibits an effect of the parameter η on the conductance spectra of the discussed setup with two equal arms, $L_1 = L_2$. Although for $\eta \sim 1$ conductance spectra are dependent on the S tip position, the variations are weak and insignificant, so we do not discuss them in the paper. More important is the principal dissimilarity between $G(V)$ curves for $\eta \ll 1$ (a characteristic similar to that for conventional N/S point contacts) and $\eta \approx 1$ (the presence of a prominent dip in the gap region together with the doubled value at zero voltage). The latter characteristic is unexpected from the viewpoint of the traditional theory of the junction spectroscopy [10] although similar anomalies have been frequently observed in point-contact spectroscopy of superconductors, see [12] and references therein. It can be that in some cases they were caused by the presence of two conducting channels (instead of a single one expected).

Since the difference between $k^e(\varepsilon)$ and $k^h(\varepsilon)$ changes with ε, the persistent currents are energy-dependent. For a symmetric setup with $L_1 = L_2$ and $H = 0$, the oppositely directed currents cancel each other, as was argued above, but the difference emerges with increasing magnetic field, see the inset in Fig. 3(a). Figure 3(b) demonstrates the evolution of the $G(V)$ curves under the magnetic field effect for the symmetric setup. Again, we can see transformation of the conductance spectra from that observed sometimes in point-contact superconductor-based measurements (solid curve) to more conventional characteristics of N–barrier–S trilayers. Comparing to results shown in Fig. 2(b), this occurs at noticeably larger fields.

4. Discussion and conclusions

Electron correlation and topology are two central issues of modern condensed matter physics. That is why the interest in materials harboring dissipation-free helical edge states whose origin is enigmatic is growing sharply. The experimental distinction between classical and quantum long-range near-surface currents as well as between topologically protected or topologically trivial states in the quantum domain is challenging because of their similarity. As known, coherent quantum systems can support charge flows that remain constant over time without dissipating energy or decaying, even deprived of any external power supplies. Such persistent currents may arise not only in superconducting and

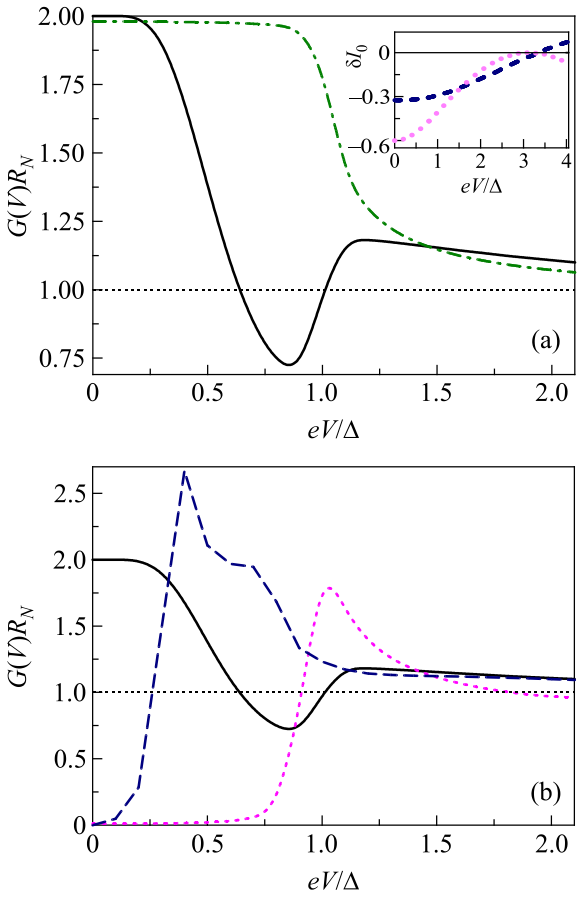

Fig. 3. (Color online) Conductance spectra $G(V)$ of a quantum loop shown in Fig. 1 without (a) and in the presence (b) of an external magnetic field **H**, $L_1 = L_2$. The difference in the Fermi momenta for electrons and holes is significant ($\eta = 1$). In related graphs, the magnetic flux Φ through the ring equals to 0, $0.01(h/2e)$, and $0.1(h/2e)$ (solid, dashed, and dotted lines, respectively), Fermi wave numbers for the metallic loop are twice those for the tips. The rest of quantities are the same as in Fig. 2. The inset demonstrates δI_0 vs V dependence for the same magnetic fluxes Φ as in Fig. 3(b).

superfluid systems but in normal conducting phases with closed paths shorter than the phase-breaking length as well. Their presence was identified by magnetometry techniques, the results of which were found to agree well with calculations based on a model of non-interacting electrons [13]. The system we propose is simpler and allows obtaining indirect confirmation of the presence of dissipationless currents by monitoring conductance spectra for different S tip positions. Application of weak perpendicular magnetic fields can address the same issue in more details. Rapid transformation of the measured $G(V)$ differential conductance from that resembling a point-contact curve to a tunneling-like characteristic and the periodicity of the effect in Φ with the period Φ_0 will provide clear-cut experimental evidence of the presence of persistent currents. Important information concerning electronic characteristics of the edge modes can be obtained by comparing the measured $G(V)$ data for different studied materials. By changing the impurity content from dopants preserving time-reversal symmetry to those violating it, we could clarify whether we are dealing with a topological matter where gapped bulk bands, characterized by a nontrivial topology, support gapless edge modes carrying dissipationless charge currents along the edges of the sample [14].

What about the practical feasibility of the discussed effects? In 1965, Sharvin and Fisher proposed and realized experimentally an idea of injecting electrons into a single crystal with a point-contact emitter and detecting them with a point-contact collector [15]. Later, it was used to prove the unconventional angular dependence of the order parameter in cuprate superconductors when the contacts were formed on different facets of a single crystal [16]. Such interferometric configuration can be realized *in situ* using a cryogenic rig for point-contact spectroscopy measurements with lateral scanning capability proposed in the work [17]. The authors of the paper [18] elaborated an independently driven double-tip scanning tunneling microscope operating under ambient conditions and successfully applied it for studying electrical transport properties of organic ultrathin films within the micrometer scale. At last, recently, an original methodology for a fine relative positioning of two independently driven point-contact tips on a surface with unprecedented atomic precision and probing distance below 50 nm was developed [19]. The two-probe experiments were carried out at cryogenic temperature of around 4.5 K with electrochemically etched tungsten tips used as probes [19]. The latter device seems to be suitable for the experiments proposed in this paper.

In conclusion, we have developed and studied the operation of a hybrid interferometric setup, a combination of two normal and superconducting scanning tips, that can be used to find out the origin of metallic-like one-dimensional edge channels in quantum materials with an insulating interior. In a simple Corbino disk geometry, the dependence of the measured differential conductance spectrum on the applied voltage bias as well as the consequences of symmetry breaking by a weak perpendicular magnetic field were analyzed. Our goal was to find the main features distinguishing a classical origin of the discussed currents from the quantum one and, in the latter case, to establish whether they are a manifestation of topologically protected states or not. We have provided detailed predictions for future experiments seeking to characterize such modes and believe that the proposed two-probe experiments with high-resolution sensing capabilities can be realized using existing techniques.

This work was supported by the joint German-Ukrainian project “Controllable quantum-information transfer in superconducting networks” (DFG project SE 664/21-1, No. 405579680 and NRFU project F81/41396).

1. S. M. Girvin and K. Yang, *Modern Condensed Matter Physics*, Cambridge University Press, Cambridge (2019).
2. J.-X. Yin, S. H. Pan, and M. Z. Hasan, *Nat. Rev. Phys.* **3**, 249 (2021).
3. D. Culcer, A. C. Keser, Y. Li, and G. Tkachov, *2D Mater.* **7**, 022007 (2020).
4. F. K. de Vries, T. Timmerman, V. P. Ostroukh, J. van Veen, A. J. A. Beukman, F. Qu, M. Wimmer, B.-M. Nguyen, A. A. Kiselev, W. Yi, M. Sokolich, M. J. Manfra, C. M. Marcus, and L. P. Kouwenhoven, *Phys. Rev. Lett.* **120**, 047702 (2018).
5. M. J. Zhu, A. V. Kretinin, M. D. Thompson, D. A. Bandurin, S. Hu, G. L. Yu, J. Birkbeck, A. Mishchenko, I. J. Vera-Marun, K. Watanabe, T. Taniguchi, M. Polini, J. R. Prance, K. S. Novoselov, A. K. Geim, and M. Ben Shalom, *Nat. Commun.* **8**, 14552 (2018).
6. A. Aharon-Steinberg, A. Marguerite, D. J. Perello, K. Bagani, T. Holder, Y. Myasoedov, L. S. Levitov, A. K. Geim, and E. Zeldov. *Nature* **593**, 528 (2021).
7. K.-J. Xu, M. Barber, E. Y. Ma, J. Xia, M. C. Hatnean, G. Balakrishnan, J. Zaanen, and Z.-X. Shen, *arXiv:2106.00112* [cond-mat.str-el] preprint.
8. E. Zhitlukhina, I. Devyatov, O. Egorov, M. Belogolovskii, and P. Seidel, *Nanoscale Res. Lett.* **11**, 58 (2016).
9. E. Zhitlukhina, M. Belogolovskii, and P. Seidel, *Appl. Nanosci.* (2021).
10. M. Belogolovskii and E. Zhitlukhina, *Junction Spectroscopy of Superconductors*, in: *A Comprehensive Guide to Superconductivity*, R. Morrow (ed.) Hauppauge, Nova Science (2021). ISBN 978-153-618-901-8.
11. A. M. Jayannavar and P. S. Deo, *Phys. Rev. B* **51**, 10175 (1995).
12. S. Volkov, M. Gregor, T. Plecenik, E. Zhitlukhina, M. Belogolovskii, and A. Plecenik, *Appl. Nanosci.* (2021).
13. A. C. Bleszynski-Jayich, W. E. Shanks, B. Peaudecerf, E. Ginossar, F. von Oppen, L. Glazman, and J. G. E. Harris, *Science* **326**, 272 (2009).
14. M. Z. Hasan and C. L. Kane, *Rev. Mod. Phys.* **82**, 3045 (2010).
15. Yu. V. Sharvin and L. M. Fisher, *Pis'ma Zh. Eksp. Teor. Fiz.* **1**, 54 (1965) [*JETP Lett.* **1**, 152 (1965)].
16. D. A. Brawner and H. R. Ott, *Phys. Rev. B* **50**, 6530 (1994).
17. M. Tortello, W. K. Park, C. O. Ascencio, P. Saraf, and L. H. Greene, *Rev. Sci. Instrum.* **87**, 063903 (2016).
18. K. Takami, S. Tsuruta, Y. Miyake, M. Akai-Kasaya, A. Saito, M. Aono, and Y. Kuwahara, *J. Phys.: Condens. Matter* **23**, 434002 (2011).
19. M. Kolmer, P. Olszowski, R. Zuzak, S. Godlewski, C. Joachim, and M. Szymonski, *J. Phys.: Condens. Matter* **29**, 444004 (2017).

Зондування протяжних струмопровідних крайових мод двома квантовими точковими контактами

M. Belogolovskii, E. Zhitlukhina, P. Seidel

Походження аномальних струмопровідних крайових станів у квантових зразках з ізолюючою внутрішньою частиною є загадковою. Запропоновано вирішити це питання за допомогою гібридного пристрою на основі двох незалежних скануючих зондів з нормальним і надпровідним вістрями, здатних реалізувати квантовий інтерференційний ефект квазічастинкових струмів, що рухаються в різних напрямках уздовж металевих одновимірних крайових каналів. Для моделювання бездисипаційних крайових струмів розглянуто квантовий матеріал з простою геометрією диску Корбіно та проаналізовано, яким чином спектр диференціальної провідності залежить від відстані між двома вістрями, прикладеної напруги та присутності магнітного поля. Суттєва різниця між класичними та квантовими очікуваннями має пояснити загадкове походження далеко протяжних провідних мод, що спостерігаються в різних матеріалах при низьких температурах. Сильна залежність від прикладеного магнітного поля може виявитись корисною для практичної реалізації досліджуваних квантових ефектів, пов'язаних з різницею фаз функцій електронних хвиль в геометрії кільця.

Ключові слова: гелікоїдальні крайові струми, диск Корбіно, двозондовий точковий пристрій, спектр диференціальної провідності.